

# Effect of microalloyed Zr on the extruded microstructure of Mg–6.2Zn-based alloys

T. Bhattacharjee,<sup>a,b</sup> T. Nakata,<sup>c</sup> T.T. Sasaki,<sup>b</sup> S. Kamado<sup>c</sup> and K. Hono<sup>a,b,\*</sup>

<sup>a</sup>Graduate School of Pure and Applied Sciences, University of Tsukuba, Tsukuba 305-8577, Japan

<sup>b</sup>National Institute for Materials Science, 1-2-1 Sengen, Tsukuba 305-0047, Japan

<sup>c</sup>Nagaoka University of Technology, 1603-1 Kamitomiokamachi, Nagaoka, Niigata 940-2188, Japan

Received 24 May 2014; revised 19 July 2014; accepted 19 July 2014

Available online 25 July 2014

The addition of a small amount of Zr to a Mg–6.2Zn (Z6) binary alloy causes a substantial increase in the tensile yield strength of the extruded form of this alloy. This is attributed to the formation of thermally stable fine Mg(Zn,Zr) precipitates, which refine the extruded microstructure. A fine dispersion of  $\beta'_1$  and  $\beta'_2$  precipitates within the refined grains after T6 aging at 160 °C results in a high tensile yield strength of 275 MPa, and an ultimate tensile strength of 318 MPa with an elongation to failure of 17.1%.

© 2014 Acta Materialia Inc. Published by Elsevier Ltd. All rights reserved.

**Keywords:** Mg–Zn alloy; ZK60; Precipitation; Transmission electron microscopy

The importance of using lightweight alloys with high specific strength in the transportation sector, as a means to reduce CO<sub>2</sub> emissions, have led to renewed interest in Mg alloys in recent years. Since Mg has a hexagonal close-packed structure with only a few slip systems, deformation processes at room temperature are difficult. Recently, additions of rare earth elements to Mg have been shown to have a beneficial effect on the deformation behavior as well as on the ductility of the Mg alloys by weakening the [0001] texture in wrought alloys [1]. Since rare earth elements are costly, there is a need to focus on low-cost alloys such as Mg–Al, Mg–Zn and Mg–Ca systems for the development of wrought alloys. An Mg–Zn-based alloy microalloyed with Zr, ZK60, has been used for industrial applications as both cast and wrought alloys. Zr is known to act as a grain refiner during casting [2–6]. However, the recent report by Oh-ishi et al. showed large differences in the extruded microstructure of the Mg–6Zn–0.4Ag–0.2Ca alloys with and without 0.6Zr (ZQX600 and ZKQX6000) [7]. ZKQX6000 had a bimodally grained microstructure with fine dispersion of Mg(Zn,Zr) precipitates, whereas ZQX600 had a uniform grain size distribution. The ZQX600 alloy in the above work con-

tained Ag and Ca, but without any Zr it showed an extruded tensile yield strength of only 153 MPa, whereas the Zr-containing ZKQX6000 alloy showed an extruded tensile yield strength of 289 MPa. The above result shows that the addition of Zr plays a major role in increasing the tensile strength of the Mg–Zn system compared to the addition of Ag and Ca.

More recently, we found that these Mg(Zn,Zr) precipitates form in a heat-treated cast ZK60 alloy [8]. The structure of the Mg(Zn,Zr) precipitate was found to be identical to  $\beta'_1$  precipitate; the former is stable up to 400 °C while the latter dissolves completely above 350 °C. This suggests that Zr works as an important alloying element to stabilize the  $\beta'_1$  phase at elevated temperature. A twin-roll cast and hot-rolled sheet of ZK60 in the T4 condition showed a tensile yield strength of 220 MPa, much higher than that of Z6, 163 MPa [9]. This suggests that the Zr-microalloyed Mg–Zn alloy ZK60 may show superior strength compared to Z6 in extruded form. Therefore, in this work, we performed an extrusion of a Mg–6.2Zn–0.6Zr (ZK60) alloy with the aim of showing the effect of the Mg(Zn,Zr) precipitates on the mechanical properties and recrystallization behavior by comparing ZK60 with a binary Mg–6.2 wt.% Zn (Z6) extruded alloy.

Alloy ingots with the compositions Mg–6.2Zn (Z6) and Mg–6.2Zn–0.6Zr (ZK60) were prepared by induction melting of high-purity Mg, Zn and Mg–34.6 wt.%

\* Corresponding author at: National Institute for Materials Science, Tsukuba 305-0047, Japan; e-mail: [kazuhiro.hono@nims.go.jp](mailto:kazuhiro.hono@nims.go.jp)

Zr master alloy in an Ar atmosphere using a steel crucible and casting into a mild steel mold. The alloy compositions and their nomenclatures are shown in Table 1 in both atomic and weight per cent. The ingots were homogenized at 350 °C for 48 h and then extruded at 350 °C with an extrusion ratio of 20:1 at a ram speed of 0.1 mm s<sup>-1</sup>. The extruded bar samples were solution treated at 400 °C for 1 h and quenched into water (T4), and then artificially aged at 160 °C in an oil bath (T6). Tensile tests of the as-extruded and T6 heat-treated samples were conducted at room temperature at an initial strain rate of  $1 \times 10^{-3}$  s<sup>-1</sup>. Electron backscattered diffraction (EBSD) analyses were carried out by using Carl Zeiss CrossBeam 1540EsB field-emission scanning electron microscope equipped with a HKL EBSD detector. Transmission electron microscopy (TEM) foils of all the samples were prepared by twin-jet electropolishing using a solution of 5.3 g LiCl, 11.6 g Mg(ClO<sub>4</sub>)<sub>2</sub>, 500 ml methanol and 100 ml 2-butoxy-ethanol at approximately -50 °C and 90 V. The specimens were surface cleaned by ion milling using a Gatan Precision ion Polishing System (PIPS) at an operating voltage of 2 kV. The microstructure was examined on a FEI Tecnai 20 TEM operating at 200 kV. The number density calculations were done as described by Underwood [10] and the thicknesses of the TEM foils were determined by convergent beam electron diffraction analysis described by Williams and Carter [11].

Figure 1 shows the tensile stress–strain curves of the Z6 and ZK60 alloys in as-extruded and peak-aged conditions. The Z6 and ZK60 alloys reach their peak hardness after 72 h of aging at 160 °C (not shown). The as-extruded Z6 alloy shows a yield strength (0.2% offset strength),  $\sigma_{ys}$ , of 162 MPa, and an ultimate tensile strength,  $\sigma_{uts}$ , of 290 MPa with an elongation to failure of 21.0%. ZK60 alloy shows a  $\sigma_{ys}$  of 254 MPa, and a  $\sigma_{uts}$  of 318 MPa in the as-extruded condition with an elongation to failure of 17.3%. Thus there is a notable difference of 92 MPa between the  $\sigma_{ys}$  of the Z6 and ZK60 alloys in

the as-extruded condition. After T6 treatment, the Z6 alloy shows a  $\sigma_{ys}$  of 244 MPa and a  $\sigma_{uts}$  of 317 MPa with an elongation to failure of 13.8%. The T6-treated ZK60 alloy shows a  $\sigma_{ys}$  of 275 MPa with a  $\sigma_{uts}$  of 318 MPa and had an elongation to failure of 17.1%.

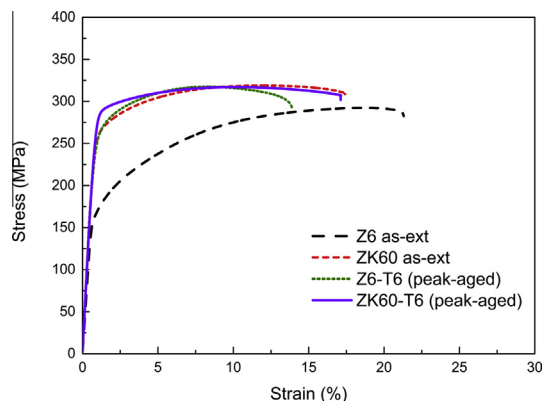
Figure 2 shows the inverse pole figure (IPF) maps of the Z6 and ZK60 alloys in the as-extruded condition from the surface perpendicular to the extrusion direction (ED). The black lines indicate grain boundaries having misorientations >15° and the white lines represent the sub-grain boundaries between 5° and 15°. The Z6 alloy shows equiaxed dynamically recrystallized grains of size  $36.0 \pm 10.0$  µm (Fig. 2a), whereas the ZK60 alloy shows a much smaller grain size with a bimodal grain microstructure, i.e. fine dynamically recrystallized grains of  $3.2 \pm 1.0$  µm along with unrecrystallized grains of 40–50 µm (Fig. 2b). In the unrecrystallized regions many sub-grain boundaries are also observed. The 10 $\bar{1}$ 0 pole figure has a weaker intensity in the Z6 alloy than in the ZK60 alloy (Fig. 2a,b). This can be attributed to the presence of the unrecrystallized grains in the ZK60 alloy which have a strong basal texture along the ED.

Figure 3 shows bright-field TEM images of Z6 and ZK60 alloys in the as-extruded condition. The Z6 alloy does not show any fine precipitates within the grains, whereas the ZK60 alloy shows a fine dispersion of precipitates in the matrix as well as along the grain boundaries (Fig. 3a,b). Some of the precipitates along the grain boundary are marked by black arrows (Fig. 3b). The precipitates are  $48.9 \pm 25.8$  nm long and  $11.6 \pm 5.6$  nm wide. Similar precipitates were also reported in a heat-treated cast ZK60 alloy in our previous work, and were Zr-rich Mg(Zn,Zr) precipitates [8].

Figure 4a–d shows the TEM bright-field images of the Z6 and ZK60 alloys aged in the T4-treated (solution

**Table 1.** The compositions and nomenclatures of the alloys used in this work.

Nomenclature	at. %	wt. %
Z6	Mg–2.4Zn	Mg–6.2Zn
ZK60	Mg–2.4Zn–0.16Zr	Mg–6.2Zn–0.6Zr



**Figure 1.** Tensile stress–strain curves of Z6 and ZK60 in as-extruded condition and in T6 (peak-aged) condition.

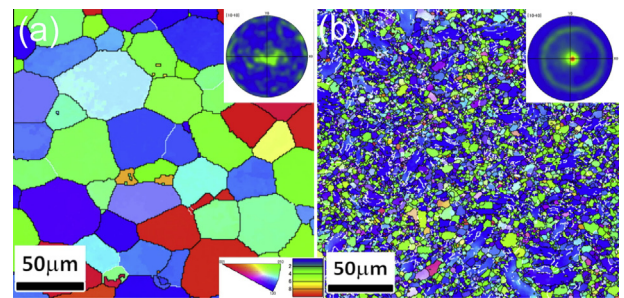


**Figure 2.** EBSD map of as-extruded (a) Z6 and (b) ZK60 alloy. The observed plane is normal to the extrusion direction.

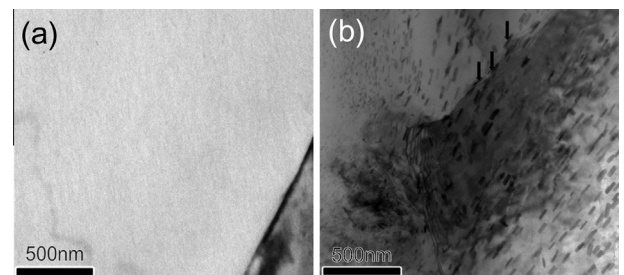


**Figure 3.** Bright-field TEM images of as-extruded (a) Z6 and (b) ZK60 alloy.

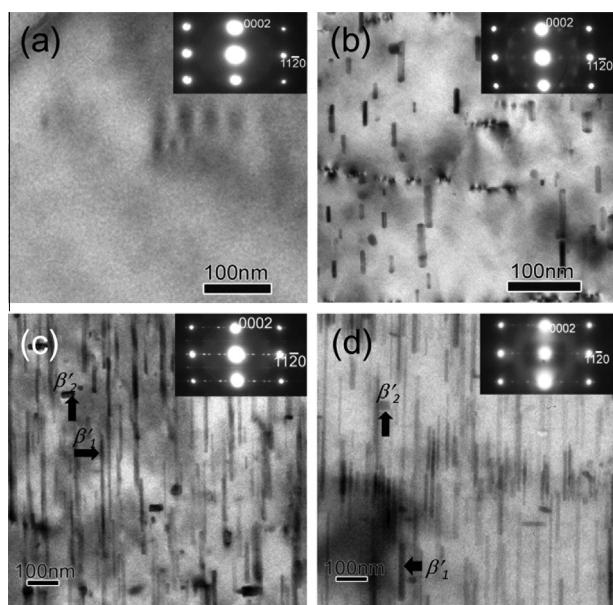


**Figure 4.** Bright-field TEM images of T4-treated (a) Z6 alloy and (b) ZK60 alloy; and peak-aged (c) Z6 alloy and (d) ZK60 alloy.

treated) and T6-treated (solution treated and artificially aged to peak-hardness) conditions. The T4-treated Z6 alloy did not show any evidence of precipitates (Fig. 4a), whereas ZK60 alloy shows fine rod-shaped Mg(Zn,Zr) precipitates (Fig. 4b) similar to that present in the as-extruded condition. The precipitates are  $52.5 \pm 24.4$  nm long and  $12.0 \pm 2.7$  nm wide, and have a number density of  $1.78 \times 10^{20} \text{ m}^{-3}$ . Therefore, we can conclude that Zr stabilizes these fine precipitates even at the elevated temperature of 400 °C. On artificial aging at 160 °C for 72 h (peak-aged condition), rod-like  $\beta'_1$  and plate-like  $\beta'_2$  precipitates form in both Z6 and ZK60 alloys as shown in Figure 4c,d. The rod-like  $\beta'_1$  precipitates in the Z6 alloy are  $223.6 \pm 118.2$  nm long and  $14.5 \pm 5.3$  nm wide, whereas the rod-like  $\beta'_1$  precipitates in the ZK60 alloy are  $221.4 \pm 112.6$  nm long and  $12.5 \pm 3.9$  nm wide in the peak-aged condition. The rod-like  $\beta'_1$  precipitates in the ZK60 alloy tend to grow along the [0001] direction of the matrix from the Mg(Zn,Zr) precipitates present in the T4 condition as they have the same  $\text{MgZn}_2$ -type crystal structure ( $P6_3/mmc$ ,  $a = 0.522$  nm,  $c = 0.856$  nm) [8]. Selected-area electron diffraction patterns indicate that the  $\beta'_1$  precipitates have an orientation relationship of  $(0001) \beta'_1 // (11\bar{2}0)_{\text{Mg}}$  and  $[11\bar{2}0] \beta'_1 // [0001]_{\text{Mg}}$  and the plate-like  $\beta'_2$  precipitates have an orientation relationship of  $(0001) \beta'_2 // (0001)_{\text{Mg}}$  and  $[11\bar{2}0] \beta'_2 // [10\bar{1}0]_{\text{Mg}}$  as previously reported [7,12]. The addition of Zr to the Z6 alloy did not alter the precipitate phases and their morphologies in the peak-aged condition.

The above results show that the tensile yield strength of the ZK60 alloy is 90 MPa larger than that of Z6 in the as-extruded condition. As seen from Figure 2a,b, there are coarse equiaxed grains in the Z6 alloy, whereas the ZK60 alloy consists of fine recrystallized grains as well as unrecrystallized grains. The unrecrystallized grains which have a strong basal texture along ED tend to have a higher resistance against yielding during tensile test [13]. The bright-field TEM micrographs also show that

there are fine Mg(Zn,Zr) precipitates in the extruded state of the ZK60 alloy, whereas no such fine precipitates were observed in the Z6 alloy (Fig. 3a,b). Our previous investigations on cast alloys also showed that the binary Mg–Zn alloy is completely solutionized at 350 °C [8]. Thus the increased tensile yield strength of the ZK60 alloy compared to the Z6 alloy in the as-extruded condition can be attributed to the bimodal microstructure developed by the presence of the Mg(Zn,Zr) precipitates and the dispersion of the fine Mg(Zn,Zr) precipitates. Previous work reported the presence of these precipitates in a heat-treated cast ZK60 alloy at 350 °C [8]. Since these precipitates are present before extrusion they tend to affect the flow behavior of ZK60 alloy during extrusion by pinning dislocations and promoting sub-grain formation in the interior of the grains. This can be seen by the formation of unrecrystallized grains in the microstructure which have misorientations of  $<15^\circ$  marked by white lines in Figure 2b. These precipitates also tend to prevent grain growth of the fine recrystallized grains [7]. This gives rise to their characteristic bimodal microstructure. Earlier work by Doan and Ansel reported a fine-grained microstructure in an extruded ZK60 alloy but this had not been linked to the presence of the Mg(Zn,Zr) precipitates [14]. Although the work by Oh-ishi et al. linked the bimodal microstructure to the presence of fine Mg(Zn,Zr) precipitates in ZKQX6000 alloy containing Ag and Ca [7], the unique role of Mg(Zn,Zr) was not established as the association between Ag and Ca was considered to be essential. On the other hand, this work has clarified that Zr is the critical element for the formation of the Mg(Zn,Zr) precipitates, which play a major role in the recrystallization behavior and tensile strength enhancement. On peak aging at 160 °C, the tensile yield strength further increases to 275 MPa in the ZK60 alloy due to the increase in the aspect ratio of the  $\beta'_1$  precipitates compared to the Mg(Zn,Zr) precipitates in the as-extruded condition. As the microalloyed Ag and Ca substantially refine the  $\beta'_1$  precipitate and increase their number density, Ag and Ca microalloying is effective at enhancing the yield strength further to 325 MPa [7], but its increment is only minor. This work has shown that the role of Zr in recrystallization behavior is very significant for producing a high yield strength, and hence ZK60, which is free from expensive Ag, has a strength nearly equivalent to that of ZKQX6000.

Homma et al. reported that their extruded Mg–6.6Zn–0.19Ca (ZX) alloy had a tensile yield strength of only 148 MPa, and Oh-ishi et al. reported an extruded tensile yield strength of 153 MPa in their ZQX600 alloy [7,13]. The extruded Z6 alloy in the present work shows a similar tensile yield strength of 162 MPa. These results show that the addition of Ag and Ca without Zr to binary Mg–Zn alloy is not effective in increasing the tensile yield strength in the as-extruded conditions. The addition of Zr makes the  $\beta'_1$  ( $\text{MgZn}_2$ ) precipitates thermally stable at the extrusion temperature by incorporation of Zr, thereby attaining a tensile yield strength of  $>250$  MPa. Ca and Ag do not alter the recrystallized microstructure as Zr does. The effect of Ca and Ag is to enhance the kinetics of the precipitation of  $\beta'_1$  to further increase the yield strength of ZK60 by artificial aging.



In summary, these microstructural studies show that extruded as well as T4-treated ZK60 alloy shows fine Mg(Zn,Zr) precipitates, whereas the Z6 alloy does not. The addition of Zr plays a critical role in stabilizing Mg(Zn,Zr) precipitates, giving rise to a bimodal microstructure in the ZK60 alloy and a corresponding difference of 92 MPa in the tensile yield strength in the as-extruded condition compared to Z6 alloy. On peak aging of the ZK60 alloy at 160 °C for 72 h, a tensile yield strength of 275 MPa, and an ultimate tensile strength of 318 MPa with an elongation to failure of 17.1% were obtained due to the increase in the aspect ratio of the  $\beta'_1$  precipitates compared to the Mg(Zn,Zr) precipitates in the as-extruded condition.

One of the authors (T.B.) acknowledges the National Institute for Materials Science (NIMS) for the provision of a NIMS Junior Research Assistantship. This work was supported by MEXT, Grant-in-Aid for Scientific Research on Innovative Areas on “Bulk Nanostructured Metals” and JST, ALCA.

- [1] N. Stanford, M.R. Barnett, *Mater. Sci. Eng. A* 496 (2008) 399.
- [2] E.F. Emley, *Principles of Magnesium Technology*, Pergamon Press, Oxford, 1966.

- [3] Y. Tamura, N. Kono, T. Motegi, E. Sato, *Jpn. Inst. Light Metal.* 47 (1997) 679.
- [4] Y.C. Lee, A.K. Dahle, D.H. St. John, *Metall. Mater. Trans. A* 31 (2000) 2895.
- [5] M. Qian, D. H. St. John, M. T. Frost, in H. I. Kaplan (Ed.), *Magnesium Technology 2003*, TMS, Warrendale PA, 2003, p. 209.
- [6] D.H. StJohn, M. Qian, M.A. Easton, P. Cao, Z. Hildebrand, *Metall. Mater. Trans. A* 36 (2005) 1669.
- [7] K. Oh-ishi, C.L. Mendis, T. Homma, S. Kamado, T. Ohkubo, K. Hono, *Acta Mater.* 57 (2009) 5593.
- [8] T. Bhattacharjee, C.L. Mendis, T.T. Sasaki, T. Ohkubo, K. Hono, *Scripta Mater.* 67 (2012) 967.
- [9] T. Bhattacharjee, B.-C. Suh, T.T. Sasaki, T. Ohkubo, N.J. Kim, K. Hono, *Mater. Sci. Eng. A* 609 (2014) 154.
- [10] E.E. Underwood, *Quantitative Stereology*, Addison Wesley, Reading, MA, 1970.
- [11] D.B. Williams, C.B. Carter, *Transmission Electron Microscopy*, second ed., Springer, New York, 2009.
- [12] J. Gallot, R. Graf, *Comptes. Rendus. Acad. Sci.* 261 (1965) 728.
- [13] T. Homma, C.L. Mendis, K. Hono, S. Kamado, *Mater. Sci. Eng. A* 527 (2010) 2356.
- [14] J.P. Doan, G. Ansel, *Trans. AIME* 171 (1947) 286.